

Structural and electronic interaction at CuO-hexa-*peri*-hexabenzocoronene hybrid interface

Bharti Singh,¹ B. R. Mehta,^{1,a)} M. Singh,¹ Govind Gupta,² L. Dössel,³ X. Feng,³ and K. Müllen³

¹*Thin Film Laboratory, Department of Physics, Indian Institute of Technology Delhi, New Delhi 110016, India*

²*Surface Physics Group, National Physical Laboratory (CSIR), New Delhi 110012, India*

³*Max-Planck Institute for Polymer Research, D-55128 Mainz, Germany*

(Received 16 November 2010; accepted 4 January 2011; published online 14 February 2011)

Interfacial interaction at hybrid interfaces results in structural and electronic properties different from organic and inorganic components. In this study, x-ray photoelectron spectroscopy analysis carried out on CuO-hexa-*peri*-hexabenzocoronene (HBC) bilayers shows the appearance of an additional C 1s peak at lower energy due to Cu–C interaction. Spectroscopic ellipsometry investigation shows that interfacial layer (~4 nm) has absorption features related to Cu–C bonding, modified HBC valence states, and Cu²⁺- π electron interaction. The observed resistive switching property of the CuO-HBC layers is considerably different from junction properties of HBC and CuO layers and is directly related to the hybrid interfacial layer. © 2011 American Institute of Physics. [doi:10.1063/1.3544937]

Understanding the interfacial properties of an organic-inorganic (OI) hybrid junction is scientifically challenging due to large dissimilarities in the structural and electronics nature of the two materials.¹ Recent reports suggest that hybrid interfaces will open up possibilities for devices such as organic light emitting diodes, thin film field-effect transistors, and photovoltaic devices.^{2–5} By controlling the properties of organic and inorganic layers, the interfacial properties of the hybrid interfaces and the device characteristics can be fine tuned and controlled.

This letter reports the study of the interface between inorganic CuO semiconductor and organic hexa-*peri*-hexabenzocoronene (HBC) layers and the effect of hybrid interfacial layer on the optical and resistive switching properties. HBC is a well known planar polycyclic aromatic hydrocarbon molecule and can be regarded as disk-shaped hydrogen terminated graphene fragment, having delocalized electrons on both sides of the molecular plane. HBC molecules segregate themselves into columnar superstructures due to π - π interactions of the aromatic cores. It is known to exhibit high intrinsic charge carrier mobilities of up to 1 cm²/V s in its bulk form with a highest occupied molecular orbital and lowest unoccupied molecular orbital (LUMO) gap of 2.8 eV.⁶ HBC layer has been used as promising interfacial layer for increasing open circuit voltage of GaAs based Schottky barrier solar cells.⁷ On the other hand, CuO is a p-type inorganic semiconductor having monoclinic structure with an optical band gap of 1.2 eV.⁸ The hole mobility of CuO is 0.1 cm²/V s. CuO has excellent photovoltaic, electrochemical, and catalytic properties.⁹ The central objective of this study is to investigate the structural and electronic changes at the CuO-HBC heterointerface for understanding the switching mechanism in a bilayer resistive memory device.

In this study, deposition of thin organic layer of HBC (~20 nm) onto the copper base has been carried out using thermal evaporation technique. The synthesis of HBC is described elsewhere.¹⁰ A thin film of CuO (~400 nm) was deposited over HBC layer using rf-magnetron sputtering from a Cu₂O target (99.99% purity). The sputtering was carried out at room temperature with an applied rf power of 100 W. Thereafter, a titanium top electrode (~100 nm) was deposited using thermal evaporation technique through a shadow mask onto the copper oxide layer. Junction properties of Ti-CuO-HBC (20 nm)-Cu have been studied using 6517-A electrometer from Keithley, Ohio.

X-ray photoelectron spectroscopy (XPS) was carried out using an ultra high vacuum XPS system (Model 1257) from Perkin Elmer, Minnesota. The Cu-HBC and CuO-HBC sample for XPS studies were prepared by depositing a thin layer of (~10 nm) Cu and CuO onto a HBC layer deposited on glass substrate. The optical properties of CuO (10 nm)-HBC sample were studied using spectroscopic ellipsometry (SE) in the wavelength range of 200–1000 nm using an M-2000F ellipsometer from J. A. Woollam Co., Inc., Nebraska.

Figure 1(a) shows the C 1s spectra of CuO-HBC, HBC, and Cu-HBC sample. It was observed that in addition to the C 1s peak at 284.6 eV observed in all samples, an additional peak at 282.7 eV is observed in the case of the CuO-HBC sample. The low intensity peak at lower energy in comparison with the main C 1s peak indicates interaction at the CuO-HBC hybrid interface. Electronegativity difference between Cu (1.9) and C (2.5) results in charge transfer from Cu to C, causing an additional C 1s peak at lower binding energy corresponding to a Cu–C bond. In a similar study, fluorine groups have been shown to influence the electronic properties of HBC and the higher electronegativity of F (4.1) with respect to C resulted in electron transfer from C to F, which shifts the C 1s peak toward higher binding energy by about 2 eV.¹¹ A similar shift in binding energy has been explained due to the interface polarization of the valence

^{a)}Author to whom correspondence should be addressed. Electronic mail: brmehta@physics.iitd.ac.in.

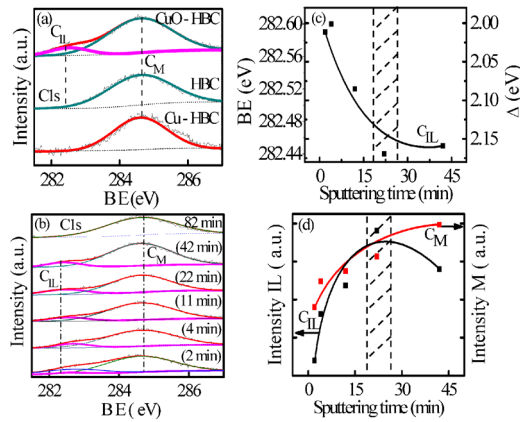


FIG. 1. (Color online) (a) C 1s peak in CuO-HBC, HBC, and Cu-HBC sample. (b) Variation of C 1s peak position in CuO-HBC sample with depth profiling showing two C 1s peaks [main peak (C_M) at 284.60 eV corresponding to HBC and interfacial layer (C_{IL}) peak]. (c) Variation of binding energy (BE) and deviation (Δ) from the C_M peak for C_{IL} peak in CuO-HBC sample with depth profiling. (d) Intensity variation of C_M and C_{IL} peak with depth profiling.

density of states in Be/W system.¹² To study the changes in C 1s spectra across the hybrid interface, XPS depth profiling was carried out for CuO-HBC sample and the results are presented in Fig. 1(b). It was observed that the binding energy of the interfacial peak (C_{IL}) decreases and the difference (Δ) between C_{IL} and the main peak (C_M) increases as one moves toward the interface up to about 20 min of sputtering [Fig. 1(c)]. The intensity of the C_{IL} peak is observed to increase up to 20 min of sputtering, whereas the intensity of the C_M peak at 284.6 eV follows the opposite trend and continues to increase [Fig. 1(d)]. These results show that sample depth at 15–25 min of sputtering corresponds to the interfacial region [shown by the shaded portion in Figs. 1(c) and 1(d)].

Spectroscopic ellipsometry was carried out onto CuO-HBC sample. The best fit to the experimental data in terms of ellipsometric angles (Ψ) was obtained by incorporating an interfacial region of (~ 4 nm) in the CuO-HBC structure. Thickness and optical constants of the CuO top layer (TL), interfacial layer (IL), HBC bottom layer (BL) was obtained by fitting of the experimental data at three different incident angles using a four layer (CuO-IL-HBC-glass substrate) optical model. The absorption coefficient (α) versus energy ($h\nu$) plots for the top, bottom, and interfacial layers are shown in Fig. 2(b)–2(d), respectively. It was observed that the absorption spectra corresponding to HBC BL exhibits two peaks (marked as 3' and 4') and the IL absorption spectra show five peaks marked as (1, 2, 3, 4, and 5) [Figs. 2(c) and 2(d)]. This implies that the interface region has a number of distinct features in terms of absorption spectra. Electronic interaction between CuO and HBC in the interfacial region results in the appearance of additional peaks in the absorption spectra. The peak position in the absorption spectra for the HBC BL (3' and 4') and IL (1, 2, 3, 4 and 5) obtained is summarized in Table I. Peaks 3' and 4' observed at 2.75 and 3.5 eV in the absorption spectra of HBC BL are related to the I and II valence levels of HBC. A careful analysis of the peak position in the absorption spectra of the interfacial layer points toward its hybrid nature. Peaks 1 and 2 at 2.03 and 2.5 eV seems to be related to the band-to-band transition of Cu_2C_2 or Cu_2C_4 normally observed between 1.5 to 2.0 eV.¹³

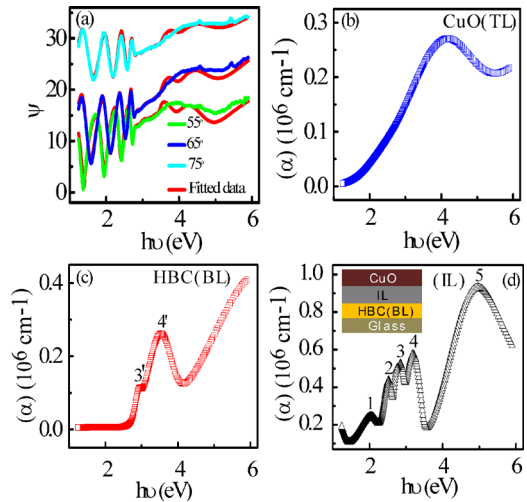


FIG. 2. (Color online) (a) Experimental and modeled ellipsometric angles " Ψ " for CuO-HBC sample at three different incident angles of 55°, 65°, and 75° using four layer optical model [see inset of (d)]. Absorption spectra (α) for (b) CuO TL, (c) HBC BL, and (d) IL.

Peak positions marked as 3 and 4 correspond to modified I and II valence levels of HBC. Peak positions marked as 5 seem to be related to interaction of cation (Cu^{2+}) with the π electron of aromatic chains of HBC. A similar absorption feature due to cation- π electron has been presented in Cu^{2+} -tryptophan system.¹⁴ Thus, the optical absorption spectra of the interfacial layer show structural and electronic interaction between the organic and inorganic components.

As the resistive switching phenomenon is known to be extremely sensitive to interfacial properties,¹⁵ the effect of interfacial interaction on CuO-HBC hybrid interface has been studied by investigating resistive switching properties. For observing resistive switching phenomenon, an electroforming voltage is applied to metal-insulator-metal (MIM) structure, which results in a large change in resistance. Subsequently, the MIM structure can be switched from low resistance state (LRS) to high resistance state (HRS) upon application of reset point voltage (V_R) and back to LRS on application of set point voltage (V_S).¹⁶ If the LRS and HRS occur at the same voltage polarity, switching is referred to as unipolar; otherwise, bipolar.

Figure 3(a) shows the electroforming process performed on the pristine Ti-CuO-HBC-Cu structure with a current compliance limit of 2 mA on applying a voltage of 0.44 V. After electroforming, the Ti-CuO-HBC-Cu cell remains in the LRS and exhibits linear I-V characteristics up to a volt-

TABLE I. Comparison of peak position in absorption spectra for the HBC BL and IL with ultraviolet photoelectron spectroscopy results for the HBC sample (see Ref. 6). E_α HBC (BL) and E_α (IL) correspond to the peak position in the absorption spectra for BL and IL, respectively, whereas E_{FL} and E_{LUMO} correspond to position of valence states with respect to the Fermi level and the lowest unoccupied molecular orbital.

E_α HBC (BL) (eV)	E_α (IL) (eV)	E_{FL} (eV)	E_{LUMO} (eV)	Peak assignment
...	2.03	Cu_2C_2
...	2.51	Cu_2C_4
2.75	2.85	1.35	2.80	First valence State (HBC)
3.50	3.20	1.75	3.20	Second valence State (HBC)
...	4.95	Cu^{2+} - π interaction

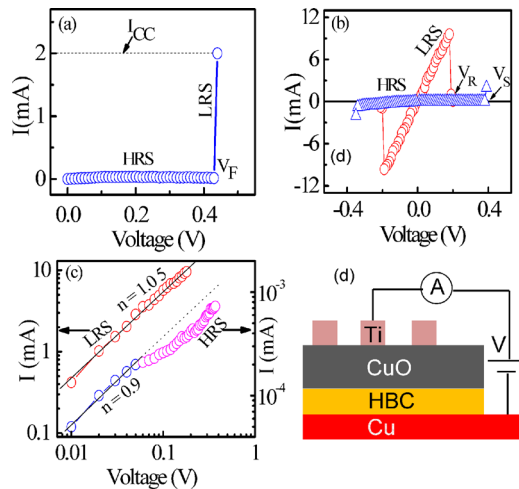


FIG. 3. (Color online) (a) Current-voltage characteristics for Ti-CuO-HBC-Cu sample during the initial electroforming step, showing transition to LRS at forming voltage (V_F) of 0.44 V with a current compliance limit (I_{CC}) of 2 mA. (b) I-V curve showing reversible and unipolar resistive switching for Ti-CuO-HBC-Cu sample. The sample switches from LRS to HRS at a reset voltage (V_R) of 0.29 V and switches back to LRS at a set voltage (V_S) of 0.39 V. (c) Double logarithmic I-V plots showing the linear Ohmic behavior with slope of about 1.05 in the LRS. Linearity is observed in HRS at lower voltages with slope of about 0.9; deviation from this linearity is observed in HRS at higher voltages. (d) Schematic diagram of the Ti-CuO-HBC-Cu structure used for studying resistive switching properties.

age of 0.19 V as shown in Fig. 3(b). Upon increasing the voltage further, the sample switches to HRS at a reset voltage (V_R) of 0.2 V. Upon further increase in voltage bias, the sample switches back to LRS state upon application of a set point voltage (V_S) of 0.39 V. The typical resistance values in LRS and HRS are observed to be ($\sim 18 \Omega$) and ($\sim 38.5 \times 10^4 \Omega$) at a voltage of 0.1 V. A high value of resistance ratio $\sim 2 \times 10^4$ between the HRS and LRS state is quite attractive from an application point of view. The resistive switching behavior was observed to be unipolar with reproducible I-V characteristics. Double logarithmic plots of the I-V curve in both LRS and HRS states are presented in Fig. 3(c). A I-V characteristic in LRS displays the Ohmic behavior with an approximate slope of 1.08. The conduction mechanism of the HRS at low voltage also follows Ohm's law, but appreciable nonlinearity is observed at high voltages. It does not seem to follow any single law and may be a combination of different possible current transport mechanisms such as trapping (detrapping) of space charge limited current and the formation (deformation) of multifilaments, as reported earlier.¹⁷ It may be noted that Ti-HBC-Cu and Ti-CuO-Cu structures showed linear and rectifying I-V characteristics, respectively (not shown here), and resistive switching behavior was observed to be completely absent. This confirms that hybrid interfacial layer is responsible for resistive switching phenomenon.

Furthermore, resistive switching characteristics of the Ti-HBC-CuO-Cu junction (not shown here) in which the HBC layer was vacuum evaporated onto a CuO layer shows higher electroforming voltage (>50 V) in comparison with (0.44 V) when the CuO layer is sputter deposited onto the HBC layer. XPS and SE results showed minimal modification at the interface in the former case (not shown here). Kinetic energy of copper or oxygen adatoms during sputter

deposition of CuO onto a HBC layer seems to be an important factor controlling the extent of interfacial interaction. The degree of interfacial interaction at CuO-HBC hybrid junction can be controlled by changing the energy of adatoms (sputtering voltage or deposition pressure) or by post-deposition heat treatment (time and duration). Such a study will help in further understanding the nature of the interfacial layer and the resistive switching mechanism. It may be mentioned that there are a number of reports on the resistive switching behavior in organic and inorganic layers. The resistive switching properties observed in the present study are due to hybrid interfacial layer and not due to CuO and HBC layer.

In conclusion, XPS analysis carried out on CuO-HBC bilayers shows the appearance of an additional C 1s peak at lower energy due to electron transfer from Cu to C. Optical modeling based on SE data shows the formation of interfacial layer of about 4 nm thickness, with absorption features related to Cu-C bonding, modified HBC valence states, and $\text{Cu}^{2+}-\pi$ electron interaction. Electrical properties of MIM structures comprising of CuO-HBC layers show that the interfacial layer is directly responsible for the observed resistive switching properties as junctions formed from the inorganic CuO layer and the organic HBC layer shows rectifying and Ohmic characteristics, respectively. This study presents an example in which the formation of hybrid interfacial layer results in electrical properties not observed in the organic and inorganic components.

One of the authors (Bharti Singh) is thankful to the Council of Scientific and Industrial Research, India for providing junior research fellowship. The authors would like to thank Mr. Amit Chauhan for carrying out x-ray photoelectron spectroscopy measurements.

- ¹C. N. R. Rao, A. K. Cheetham, and A. Thirumurugan, *J. Phys.: Condens. Matter* **20**, 083202 (2008).
- ²J. Lee, B.-J. Jung, J.-I. Lee, H. Y. Chu, L.-M. Do, and H.-Ku. Shim, *J. Mater. Chem.* **12**, 3494 (2002).
- ³G. B. Murdoch, M. Greiner, M. G. Helander, Z. B. Wang, and Z. H. Lu, *Appl. Phys. Lett.* **93**, 083309 (2008).
- ⁴C. R. Kagan, D. B. Mitzi, and C. D. Dimitrakopoulos, *Science* **286**, 945 (1999).
- ⁵R. Zhu, C.-Y. Jiang, B. Liu, and S. Ramakrishna, *Adv. Mater.* **21**, 994 (2009).
- ⁶H. Proehl, M. Toerker, F. Sellam, T. Fritz, K. Leo, C. Simpson, and K. Müllen, *Phys. Rev. B* **63**, 205409 (2001).
- ⁷S. Özcan, J. Smoliner, T. Dienel, and T. Fritz, *Appl. Phys. Lett.* **92**, 153309 (2008).
- ⁸B. Balamurugan and B. R. Mehta, *Thin Solid Films* **396**, 90 (2001).
- ⁹N. Serin, *Semicond. Sci. Technol.* **20**, 398 (2005).
- ¹⁰M. Müller, C. Kübel, and K. Müllen, *Chem.-Eur. J.* **4**, 2099 (1998).
- ¹¹S. Entani, T. Kaji, S. Ideda, T. Mori, Y. Kikuzawa, H. Takeuchi, and K. Saiki, *J. Phys. Chem. C* **113**, 6202 (2009).
- ¹²Y. Wang, Y. Nie, L. K. Pan, Z. Sun, and C. Q. Sun, *Appl. Surf. Sci.* **257**, 3603 (2011).
- ¹³B. Balamurugan, B. R. Mehta, and S. M. Shivprasad, *Appl. Phys. Lett.* **82**, 115 (2003).
- ¹⁴H. Yorita, K. Otomo, H. Hiramatsu, A. Toyama, T. Miura, and H. Takeuchi, *J. Am. Chem. Soc.* **130**, 15266 (2008).
- ¹⁵N. Zhong, H. Shima, and H. Akinaga, *Appl. Phys. Lett.* **96**, 042107 (2010).
- ¹⁶R. Waser and M. Aono, *Nature Mater.* **6**, 833 (2007).
- ¹⁷R. Dong, D. S. Lee, W. F. Xiang, S. J. Oh, D. J. Seong, S. H. Heo, H. J. Choi, M. J. Kwon, S. N. Seo, M. B. Pyun, M. Hasan, and H. Swang, *Appl. Phys. Lett.* **90**, 042107 (2007).